

COP DEGRADATION DUE TO SUCTION SUPERHEATING IN REFRIGERATION CYCLES OPERATING WITH NON-AZEOTROPIC MIXTURES

Ricardo Fernando Paes Tiecher, ricardo.tiecher@aluno.puc-rio.br

José Alberto Reis Parise, parise@puc-rio.br

Pontifícia Universidade Católica do Rio de Janeiro, Department of Mechanical Engineering
22453-900 Rio de Janeiro RJ, Brazil

Abstract. *The present work is concerned with the development of a thermodynamic model in which condensing and evaporating temperatures, as well as compressor empirical performance, are provided individually as input data. The primary goal is to obtain efficiency parameters for non-azeotropic R-22 replacements (R-410A, R-404A and R-407C) in simple vapor compression refrigeration cycles. The effect of evaporator superheat on cycle performance is studied. Results are presented as the discharge temperature, suction pressure and COP against the degree of superheating. The midpoint approach was adopted to define nominal condensing and evaporating temperatures. Given the dependence of the heat transfer coefficient on the local governing conditions on each side of the heat exchangers, and in order to allow for a future extension of this work to UA models, a multi-zone approach was adopted.*

Keywords: *Non-azeotropic, Glide, Multi-zone, Simulation, COP degradation*

1. INTRODUCTION

Natural refrigeration goes back to ancient times. The foundation for “artificial” refrigeration, according to Calm (2008), was set in the 1600s and 1700s, when numerous investigators in different countries studied phase change physics. The first generation of refrigerants comprised well-known solvents and other volatile fluids, effectively including whatever worked and was available. Almost all of these refrigerants were flammable, toxic, or both, and some were also extremely reactive. The second generation was characterized by a shift to fluorochemicals for durability and safety (Calm, 2008). Chlorofluorocarbons (CFCs) and later hydrochlorofluorocarbons (HCFCs) commanded this era. Ammonia continued as the most popular refrigerant in large, industrial-scale systems.

As reported by Calm (2008), the association of released CFCs to the depletion of protective ozone propelled the third generation, aiming at stratospheric ozone preservation. The Montreal Protocol forced abandonment of ozone-depleting substances (ODSs). Fluorochemicals retained the primary focus, with emphasis on HCFCs and hydrofluorocarbons (HFCs).

The very successful response to ozone depletion stands in sharp contrast to the deteriorating situation with climate change. The Kyoto Protocol sets binding targets for greenhouse gas (GHG) emissions based on calculated equivalents of carbon dioxide, methane, nitrous oxide, HFCs, perfluorocarbons (PFCs), and sulphur hexafluoride, as stated in Calm (2008). More recent measures are forcing shifts to a fourth generation of refrigerants defined by attention to global warming (Pearsons, 2012).

In addition to an intensive experimental effort, a refrigerant substitution program requires a comprehensive work on the performance prediction of several different alternatives. For that purpose, simulation models can become powerful tools for refrigerant analysis. In the present thermodynamic model, condensing and evaporating temperatures, as well as compressor empirical performance, are provided individually as input data. The primary goal is to obtain efficiency parameters for selected R-22 replacements (R-410A, R-404A and R-407C) in simple vapor compression refrigeration cycles. Results are presented, for example, in terms of the discharge pressure, suction pressure, COP and entropy generation against a control variable, like the degree of superheating.

2. THERMODYNAMIC MODEL

The mathematical model is outlined below, starting with the definition of the control volumes, followed by the modeling of each component. Eight control volumes comprise the single vapor compression refrigeration cycle, namely: compressor (cp), condenser's desuperheating (ds), condensing (cs) and subcooling (sc) zones, expansion device (xd), evaporator's boiling (bo) and superheating (sh) zones, and suction line (sl).

2.1 Definition of evaporating and condensing temperatures

According to Hundy and Vitall (2000), for glide refrigerants, such as R-407C, there is a need to determine the appropriate temperatures that define suction and discharge conditions. The midpoint approach advocates the use of the temperatures that are midway the condensation and evaporation processes, as plotted in a P-h diagram. The midpoint

protocol will render a good system performance comparison with non-glide refrigerants, such as R-22, and has been widely used. Oppositely, with the dew-point protocol, the evaporating and condensing temperatures are defined at the corresponding dew points. Hundy and Vitall (2000) compare the results, in terms of compressor capacity and COP (EER) values, when the midpoint and dew point definitions are applied to specific compressor rating points.

2.2 Control volumes

Figure 1 depicts the cycle P-h diagram with control volumes and refrigerant thermodynamic states (including midpoints) in their corresponding positions. They are: compressor (cp); condenser: desuperheating (ds), condensing (cs) and subcooling (sc); expansion device (xd); evaporator: boiling (bo) and superheating (sh); suction line (sl); refrigerant states: 1 – compressor suction; 2 – compressor discharge; 3 – start of condensation (or dew point, for mixtures); 4 – condenser midpoint, for mixtures; 5 – condenser saturated liquid or, for mixtures, bubble point; 6 – condenser outlet; 7 – evaporator inlet; 8 – evaporator midpoint, for mixtures; 9 – evaporator dry-out point, 10 – suction line inlet.

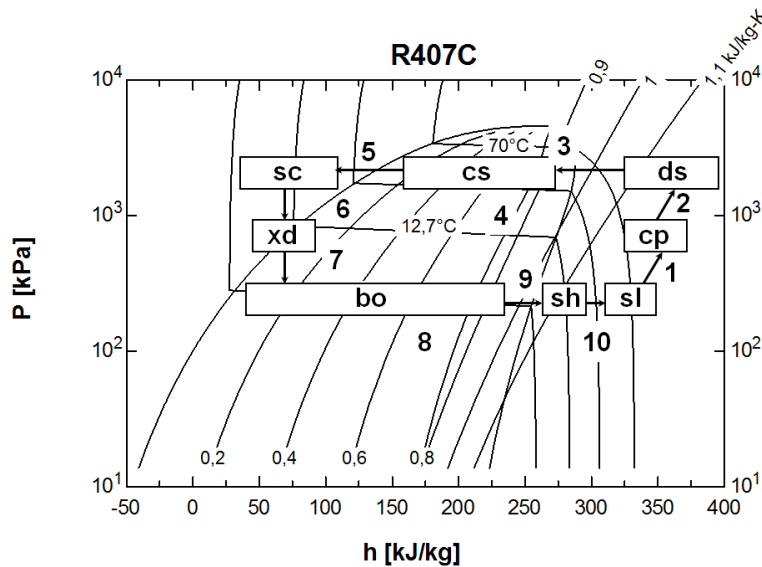


Figure 1. Control volumes and refrigerant states (including midpoints) for the mathematical model.

2.3 Compressor

A simple efficiency-based model is employed for the compressor. An empirical value is provided for the isentropic efficiency, $\eta_{s,cp}$, which is related to compressor suction and discharge thermodynamic states as follows:

$$\eta_{s,cp} = \frac{(h_{2s} - h_1)}{(h_2 - h_1)} \quad (1)$$

where h (kJ/kg) is the specific enthalpy and, below, s (kJ/kg·K) is the specific entropy and $2s$ refers to isentropic compression discharge.

$$s_{2s} = s_1 \quad (2)$$

Compressor adiabatic work, w_{cp} (kJ/kg) is calculated from:

$$w_{cp} = h_2 - h_1 \quad (3)$$

2.4 Condenser

Each zone of the condenser, Fig. 2, is treated as an independent heat exchanger, with its own energy balance equations (Martins Costa and Parise, 1993). Equations (4) and (5) describe the energy balance in the desuperheating and subcooling zones, respectively:

$$q_{ds} = h_2 - h_3 \quad (4)$$

$$q_{sc} = h_5 - h_6 \quad (5)$$

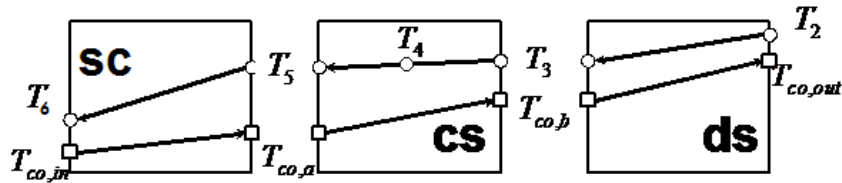


Figure 2. Control volumes (desuperheater, ds, condensing zone, cs, and subcooler, sc) for the condenser.

For the condensing zone, the following equation applies:

$$q_{cs} = h_3 - h_5 \quad (6)$$

The condenser heat, q_{cd} (kJ/kg), is:

$$q_{cd} = q_{ds} + q_{cs} + q_{sc} \quad (7)$$

$$q_{cd} = h_2 - h_6 \quad (8)$$

Finally, the prescribed condenser outlet degree of subcooling, ΔT_{sc} (K), and the mid-point protocol, T_4 (K), provide, respectively:

$$\Delta T_{sc} = T_5 - T_6 \quad (9)$$

$$T_4 = (T_3 + T_5)/2 \quad (10)$$

For convention, adopting the mid-point protocol and assuming no pressure drop, the nominal condensing pressure and the nominal condensing temperature are taken as, respectively, the pressure and the temperature at midway the condensation process (mid-point protocol, for mixtures, as stated in Hundy and Vittal, 2000), P_4 (kPa) and T_4 (K).

$$P_{cd} = P_4 \quad (11)$$

$$T_{cd} = T_4 \quad (12)$$

$$P_2 = P_{cd} \quad (13)$$

$$P_3 = P_{cd} \quad (14)$$

$$P_5 = P_{cd} \quad (15)$$

$$P_6 = P_{cd} \quad (16)$$

2.5 Expansion device

It is assumed that the expansion device is a thermostatic expansion valve which provides constant superheat, ΔT_{sh} (K), at the evaporator outlet.

$$T_{10} = T_9 + \Delta T_{sh} \quad (17)$$

Given that there is no work done and neglecting the heat transfer from the environment, from the energy conservation equation, the expansion process is isenthalpic.

$$h_6 = h_7 \quad (18)$$

2.6 Evaporator

The evaporator is treated similarly to the condenser. Two control volumes, Fig. 3, are established, dictated by the phase change of the refrigerant: boiling and superheating zones.

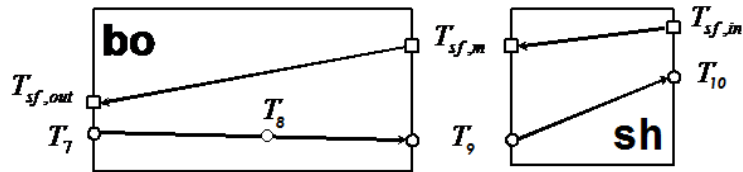


Figure 3. Control volumes (boiling, bo, and superheating, sh) for the evaporator.

The energy balance for the boiling zone is as follows:

$$q_{bo} = h_9 - h_7 \quad (19)$$

Equation (20) applies to the superheating zone:

$$q_{sh} = h_{10} - h_9 \quad (20)$$

The refrigerant effect, q_{ev} (kJ/kg), is:

$$q_{ev} = q_{bo} + q_{sh} \quad (21)$$

$$q_{ev} = h_{10} - h_7 \quad (22)$$

Likewise, the nominal evaporating pressure and the nominal evaporating temperature are taken, respectively, as the pressure and the temperature at midway the evaporation. To determine the mid-point, the average between the points at the inlet and at the outlet of the evaporator is taken, including the superheating.

$$T_8 = (T_7 + T_{10})/2 \quad (23)$$

$$P_{ev} = P_8 \quad (24)$$

$$T_8 = T_{ev} \quad (25)$$

$$P_1 = P_{ev} \quad (26)$$

$$P_7 = P_{ev} \quad (27)$$

$$P_9 = P_{ev} \quad (28)$$

$$P_{10} = P_{ev} \quad (29)$$

2.7 Suction Line

It is assumed that the suction line provides a prescribed and constant temperature rise, ΔT_{sl} (K), at the compressor inlet.

$$T_1 = T_{10} + \Delta T_{sl} \quad (30)$$

2.8 Refrigerant Properties

Equations (31) to (44), below, show property functions that calculate thermodynamic refrigerant properties, for a given thermodynamic state, as a function of two other intensive properties. They are: the specific enthalpy, \underline{h} , specific volume, \underline{v} , specific entropy, \underline{s} , temperature, \underline{T} , and pressure \underline{P} .

$$h_1 = \underline{h}(T_1, P_1) \quad (31)$$

$$v_1 = \underline{v}(T_1, P_1) \quad (32)$$

$$s_1 = \underline{s}(T_1, P_1) \quad (33)$$

$$h_{2s} = \underline{h}(s_{2s}, P_2) \quad (34)$$

$$T_2 = \underline{T}(h_2, P_2) \quad (35)$$

$$h_3 = \underline{h}(x = 1, P_3) \quad (36)$$

$$T_3 = \underline{T}(x = 1, P_3) \quad (37)$$

$$h_5 = \underline{h}(x = 0, P_5) \quad (38)$$

$$T_5 = \underline{T}(x = 0, P_5) \quad (39)$$

$$T_6 = \underline{T}(h_6, P_6) \quad (40)$$

$$T_7 = \underline{T}(h_7, P_7) \quad (41)$$

$$T_9 = \underline{T}(x = 1, P_9) \quad (42)$$

$$h_9 = \underline{h}(x = 1, P_9) \quad (43)$$

$$h_{10} = \underline{h}(T_{10}, P_{10}) \quad (44)$$

where x is the refrigerant vapor quality.

4. NUMERICAL SOLUTION

Equations (1) to (44) form a system of non-linear algebraic equations. The Engineering Equation Solver platform was employed for the numerical solution. The operation of EES, with built-in thermodynamic property functions and a powerful numerical method of solution, proved to be straightforward. In opposition to the UA model (Parise, 2010), the solution stability of this thermodynamic model was quite insensitive to prescribed guess values and upper/lower limits of the variables. Usually, convergence was achieved after a relatively short number of iterations.

5. RESULTS

As mentioned before, the main objective for the use of the thermodynamic model was to investigate the behavior of selected R-22 replacements in simple vapor compression refrigeration cycles. Prescribed values for the degree of superheating were assumed to vary, for input data purposes, uniformly from 1°C to 15°C. Therefore, the program was run to obtain variations in the discharge pressure, suction pressure, COP and entropy generation with the degree of superheating, for each refrigerant.

The refrigerants selected to be simulated were three of the blends that replace R-22: R-410A, R404A and R-407C. The following values were used as input data for the simulation: Compressor: $\eta_{s,cp} = 0,65$; Condenser: $T_{cd} = 45$ °C; $\Delta T_{sc} = 5,5$ °C; Evaporator: $T_{ev} = -32$ °C; Expansion device: thermostatic expansion valve, $\Delta T_{sh} = 5,5$ °C; Suction line: $\Delta T_{sl} = 20$ °C.

Figures 4 and 5 show the effect of the superheating on the COP and the $COP_{boiling}$, defined as:

$$COP = q_{ev}/w_{cp} \quad (45)$$

$$COP_{boiling} = q_{bo}/w_{cp} \quad (46)$$

Equation (46) is an alternative way of expressing the cycle performance, which considers, as responsible for the refrigerant effect, the boiling process alone, thus leaving the superheating zone out of the COP calculation.

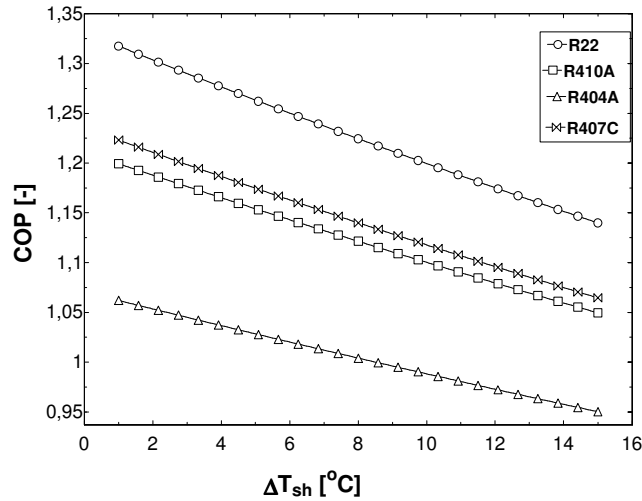


Figure 4. Effect of the degree of superheating on the cycle coefficient of performance COP , for distinct refrigerants.

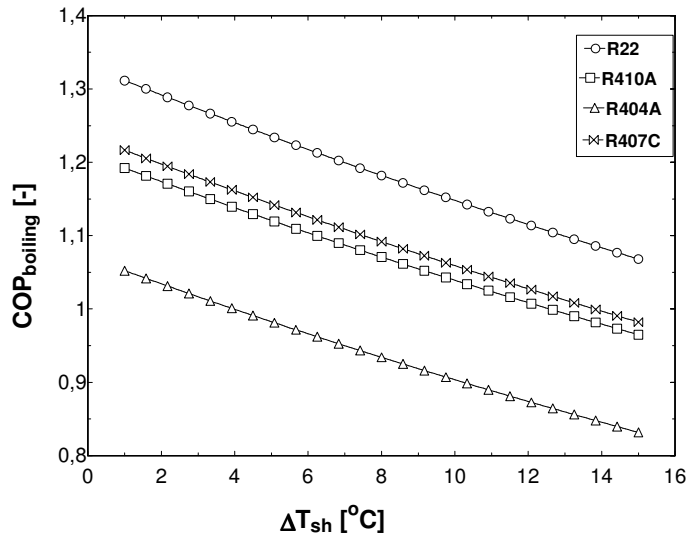


Figure 5. Effect of the degree of superheating on the cycle coefficient of performance $COP_{boiling}$, considering only the boiling zone of the evaporator as part of the refrigerant effect (that is, excluding the superheating zone from the refrigerant effect), for distinct refrigerants.

As expected, Figs. 4 and 5, higher degrees of superheating lead to a lower cycle performance (as both coefficients showed decreasing behavior). Also, the selected refrigerant affects the magnitude of both the COP and the $COP_{boiling}$. R-22 is the substance for which cycle performance is most satisfactory, followed by R-407C, R410A and R404A, respectively.

Figures 6 and 7 show the effect of the superheating on ratios $\frac{COP}{COP_{1^{\circ}C}}$ and $\frac{COP_{boiling}}{COP_{boiling; 1^{\circ}C}}$, defined as:

$$\frac{COP_{\Delta T_{sh}}}{COP_{1^{\circ}C}} = \frac{q_{ev}/w_{cp}}{q_{ev}^*/w_{cp}^*} \quad (47)$$

$$\frac{COP_{boiling; \Delta T_{sh}}}{COP_{boiling; 1^{\circ}C}} = \frac{q_{bo}/w_{cp}}{q_{bo}^*/w_{cp}^*} \quad (48)$$

where q_{ev}^* , q_{bo}^* and w_{cp}^* refer to a superheating of precisely $1^{\circ}C$.

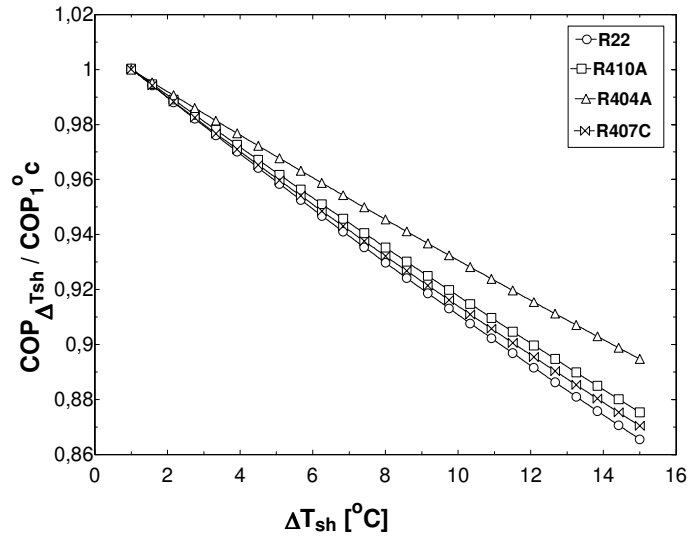


Figure 6. Effect of the degree of superheating on ratio $\frac{COP}{COP_{1^\circ C}}$, for distinct refrigerants.

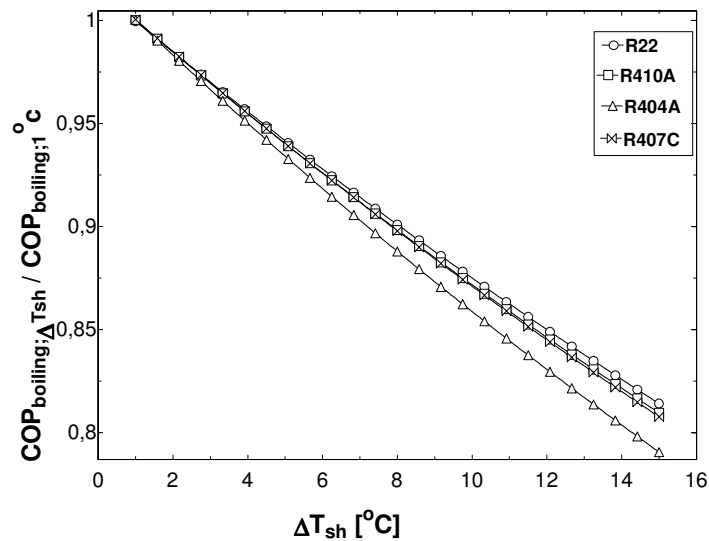


Figure 7. Effect of the degree of superheating on $COP_{boiling}$ to $COP_{boiling;1^\circ C}$ ratio, for distinct refrigerants.

As depicted in Figs. 6 and 7, the ratios $\frac{COP}{COP_{1^\circ C}}$ and $\frac{COP_{boiling}}{COP_{boiling;1^\circ C}}$ drop when the degree of superheating increases, a phenomenon known as COP degradation. However, when considering the vapor superheating as part of the refrigerant effect ($\frac{COP}{COP_{1^\circ C}}$), R-22 is the refrigerant with the highest decline in its ratio of COPs, while the curve for R-404A is the one that shows the lowest dip. On the opposite, for the refrigerant effect consisting of the boiling process alone ($\frac{COP_{boiling}}{COP_{boiling;1^\circ C}}$), the curve related to R-22 is the one that declines the least, whereas the tendency for R-404A is the most severe of all the fluids.

Figure 8 shows the effect of the superheating on the compressor suction pressure.

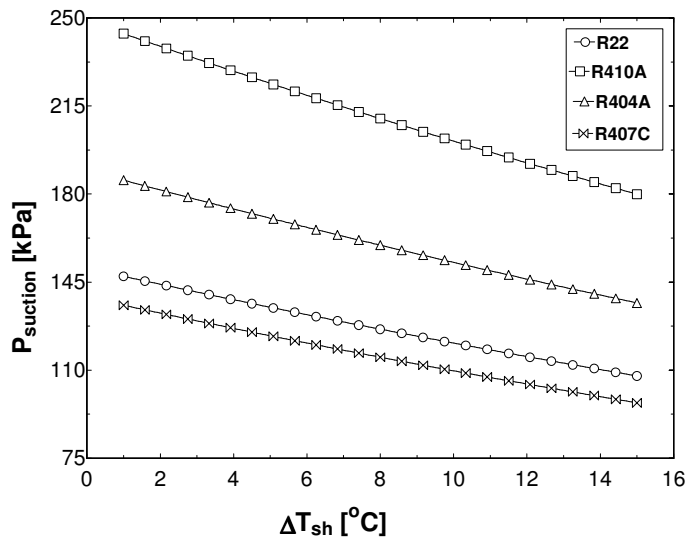


Figure 8. Effect of the degree of superheating on the compressor suction pressure, for distinct refrigerants.

As expected, similar trends were found, Fig. 8, when similar variations were applied to study the effect of the superheating on the suction pressure, this time with an observed decrease in the value of P_1 , due to the increase in the degree of superheating. Figures 9 and 10 show the effect of the superheating on the entropy generated at the compressor (Fig. 9) and the expansion device (Fig. 10), defined as:

$$s_{gen,cp} = s_2 - s_1 \tag{49}$$

$$s_{gen,xd} = s_7 - s_6 \tag{50}$$

since both processes are taken as adiabatic.

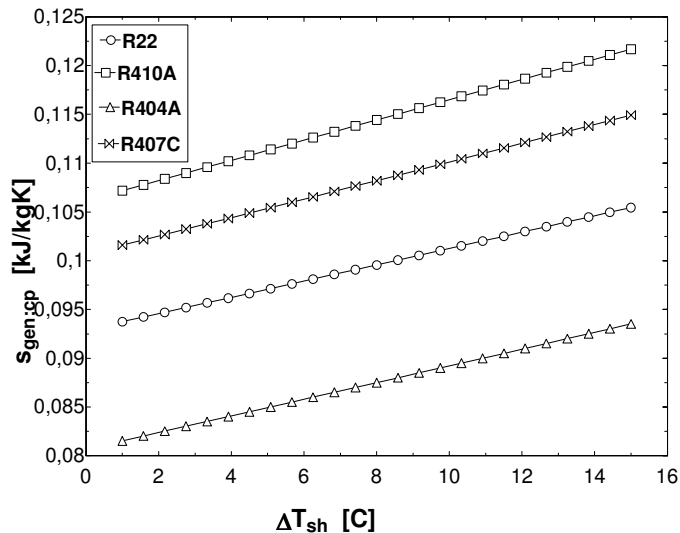


Figure 9. Effect of the degree of superheating on the specific entropy generated at the compressor, for distinct refrigerants.

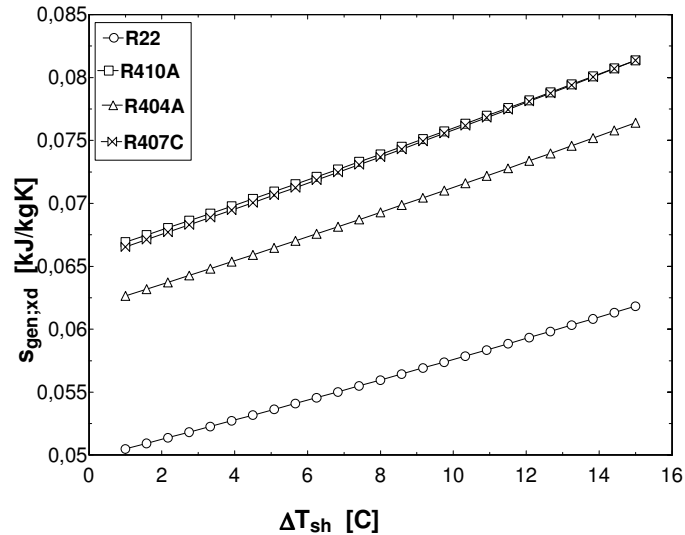


Figure 10. Effect of the degree of superheating on the specific entropy generated at the expansion valve, for distinct refrigerants.

As depicted in Figs. 9 and 10, the entropy generated was higher for increasing superheating at both control volumes. Moreover, when considering the irreversibility associated with the corresponding refrigerant, R-410A is the one with the highest entropy generation values, while the curves for R-22 and R-404A are, for Figs. 9 and 10 respectively, the ones that show the lowest results. Finally, the rate at which the entropy generated increases with the degree of superheating is approximately constant for the different mixtures considered.

6. CONCLUSIONS

In the thermodynamic model, condensing and evaporating temperatures along with compressor empirical performance were applied as input data. The foremost goal was to obtain efficiency parameters for R-22 replacement options, such as R-410A, R-404A and R-407C, in simple vapor compression refrigeration cycles. Results were presented in terms of the compressor suction pressure, the COP and the entropy generation against the degree of superheating. In spite of its relative simplicity, the model demonstrated its usefulness, particularly in parametric analyses, where the effect of basic prescribed characteristics can be assessed. This program can also serve as a basis for a more detailed simulation effort.

It was observed that, for most cases, a higher degree of superheating affects negatively the cycle performance. However, the analysis for different refrigerants indicated that the changes in values of COP and other parameters, such as suction and discharge pressures, due to the degree of superheating, are specific for each substance. Moreover, the 2nd law analysis provided interesting results associated with the increase of entropy generation at certain processes, which revealed patterns related to the specific refrigerants as well. Therefore, it is imperative to select the R-22 replacement mixture that is most suitable to the desired application for the system.

Finally, it is worthwhile to mention that this work can be extended to the development of an UA model, given the detailed description provided, especially regarding the multi-zone simulation. This progress has already been reported in Tiecher (2011).

7. ACKNOWLEDGEMENTS

Thanks are due to CAPES, CNPq and FAPERJ, Brazilian research funding agencies, for the financial support. The authors are indebted to Dr. Samuel Yana Motta, for his contributions to the project, and also to Dr. Elizabet Vera Becnerra and Eng. Paul Ortega Sotomayor, for their suggestions regarding the model, as it continued to mature over time.

8. REFERENCES

- Calm, J. M., 2008, The next generation of refrigerants, Bulletin of the IIR, International Institute of Refrigeration (IIR), Paris, 2008(1):4-10.
- Hundy, G. and Vittal, R., 2000, Compressor performance definition for refrigerants with glide, Eighth International Refrigeration Conference at Purdue University, July 25-28, West Lafayette, USA.

- Martins Costa, M. L. and Parise, J. A. R., 1993, A three-zone simulation model for air cooled condensers, *International Journal of Heat Recovery Systems & CHP*, vol. 13, n. 2, pp. 97-113.
- Parise, J. A. R., 2010, A seven-control volume simulation model for the vapour compression refrigeration cycle, *Mercofrio 2010 – Congresso de Climatização e Refrigeração*, October 20-23, Porto Alegre, Brazil.
- Pearsons, A., History of refrigerants, Short Course on “Update on refrigerants – Learning from the past, looking to the future”, *Purdue University*, July 14-15.
- Tiecher, R. F. P., 2011, Simulation of refrigeration cycles operating with non-azeotropic mixtures, *Pontifícia Universidade Católica do Rio de Janeiro, Departamento de Engenharia Mecânica, Projeto de Graduação*, Rio de Janeiro, Brazil.

9. RESPONSIBILITY NOTICE

The authors are the only responsible for the printed material included in this paper.